Journal of Applied Sciences

ISSN 1812-5654

Journal of Applied Sciences 9 (16): 2887-2896, 2009
ISSN 1812-5654

Radio Coverage inside Tunnel Utilizing Leaky Coaxial Cable Base Station

[1]F. Sayadi, [1,2]M. Ismail, [1,2]N. Misran and [1,2]K. Jumari
[1]Department of Electrical, Electronic and Systems Engineering,
[2]Institute of Space Science (ANGKASA), Level 2,
Faculty of Engineering and Built Environment Building, Universiti Kebangsaan Malaysia,
43600 UKM Bangi, Selangor Darul Ehsan, Malaysia

Abstract: In this study, tunnels radio coverage utilizing leaky coaxial cable has been described. This cable can be deployed as a base station antenna for indoor wireless system such as tunnels. The older type of leaky cables is called coupled mode, while latest type is called radiation mode. These two modes can be distinguished by their radiation pattern, method of radiation (i.e., wave or energy) and class of slot on outer conductor. To obtain the field radiation patterns, we use two models; diffuse and deterministic models. Then a modified ray tracing algorithm has been used and simulated to predict radio coverage in tunnels by leaky cable deployment. Simulations show that leaky cables achieve better RF coverage than distributed antennas in term of received signal level versus frequency for various lengths and cross section of tunnels.

Key words: Leaky coaxial cable, propagation models, ray tracing, angular resolution of rays

INTRODUCTION

Electromagnetic waves propagation in tunnel has inadmissible quality due to high scattering and multipath effect of receivable signal (Kim *et al*., 2003). Leaky cables deployment in for tunnels coverage is preferred due to some difficulties in using distributed antenna (Addamo *et al*., 2008). This cable permits implementation as a signal transmission line and antenna of electromagnetic waves by slotting on its outer conductor. There are various radio services in closed and underground environments can such as mobile communication (GSM, PCN/PCS, DECT) in building, radio coverage in parks and large multi floor buildings, mines and others, rapid emergency communication service on road in critical conditions and radio coverage of railway and metro tunnels. This study considers a novel implementation of the Ray Tracing algorithm to predict radio coverage in tunnels via., leaky coaxial cable deployment and a hybrid method that modifies the coupling between the cable and a complex environment as tunnels. Present model allows improving a method of the angular rays resolution (i.e., based on transmitted and threshold powers) resulting in intense criterion of ray tracing termination and smoother electric field coverage. Radio communication in tunnel by leaky cable deployment is shown in Fig. 1. The antenna in tunnel entrance is used for receiving signal from transmitter via., free space and its transmission in tunnel by leaky cable (Yamaguchi *et al.*, 1985).

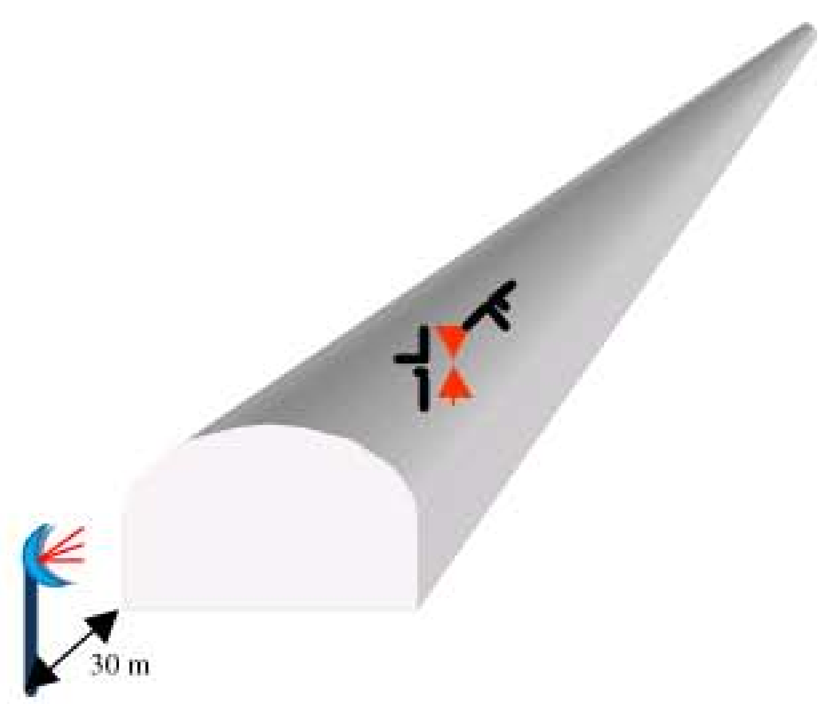

Fig. 1: Radio communication in tunnel by leaky coaxial cable deployment

LEAKY COAXIAL CABLE

Electromagnetic waves are propagated as TEM wave within coaxial cable. The wave is surrounded within the coaxial cable due to existence of outer conductor.

Corresponding Author: Fares Sayadi, Department of Electrical, Electronic and Systems Engineering, Faculty of Engineering and Built Environment, National University of Malaysia, 43600 UKM Bangi, Selangor Darul Ehsan, Malaysia Tel: +60 (3) 8921 6300/6312 Fax: +60 (3) 8921 6146

However, the electromagnetic radiations are not influenced by the propagated wave within the coaxial cable similar to the electromagnetic fields environment.

Some of the electromagnetic energy leaks from cable to environment or vice versa due to existence of slots on the outer conductor. The slots are expected to have the capability of adjusting the coupling between the cable and the environment and give smoother electric field coverage. Radio communication quality depends on amount of electromagnetic field intensity, installation method and environmental condition around of the cable. Most of tunnels comprise metallic conductors such as power transmission lines, rail and water pipes. Hence, the electromagnetic fields due to metallic's characterize are variation within tunnel. Nowadays, the cables 75 Ω are replaced by 50 Ω cables.

Two important parameters of leaky cables are cable attenuations or longitudinal attenuation and coupling attenuations. The coupling attenuations determine the ratio of radiated signal level (i.e., from the leaky cable to received signal level) by a λ/2 dipole antenna or λ/4 monopole at a specific distance from the cable. These two parameters also fluctuate according to the locations of cable, distance and situation of the slots in relation to the wall of tunnel.

Leaky cables are divided into two models (i.e., radiating and coupled) as shown in Fig. 2. In the radiating mode, the electrical field is generated by slots that are located on the outer conductor of the cable as shown in Fig. 3. The distance between slots is considered near wavelength of the radiating field of the cable. Radiation mechanism of the cable that includes slots on outer conductor is equal to an array of magnetic dipoles that are located in the length of cable.

Typically, the distance between slots is considered equal to half wavelength of radiation signal. The direction of radiation filed is radial component in this mode. In the coupled mode, the distance of slots is very much smaller than wavelength. Hence, the electromagnetic fields are scattered due to electromagnetic induction (i.e., of an external mode) on the outer conductor of the cable. Consequently, current is inducted on the outer conductor and the cable radiates similar to the traveling wave antenna. Therefore, coupled mode cable is equivalent to a long electrical antenna. The radiation pattern of electrical field can be model as diffuse and deterministic models. These models are detailed briefly in following.

Diffuse model: In this model, we assume that the radiation diffuses through a cylindrical surface of some radius larger than the physical radius of the cable, but smaller than the distance to the receiver. The power flow per unit

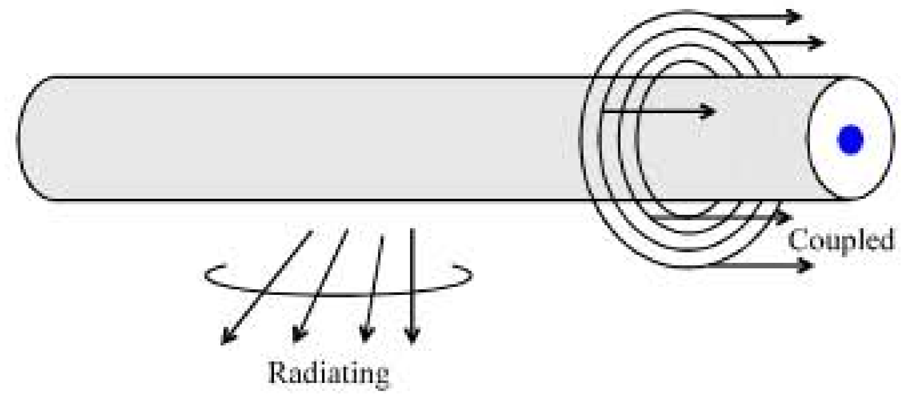

Fig. 2: Modes for the leaky cable: radiating mode and coupled mode

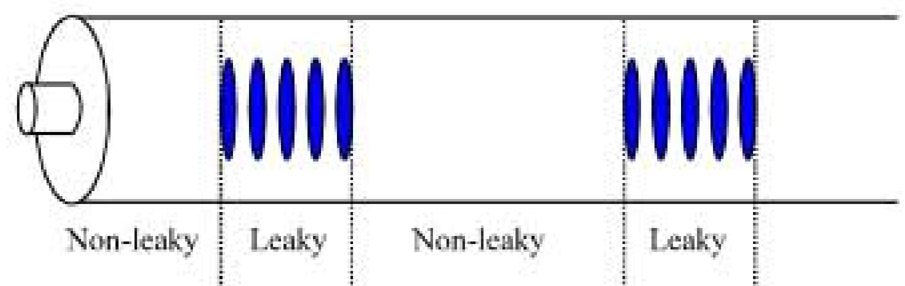

Fig. 3: Configurations of leaky coaxial cables

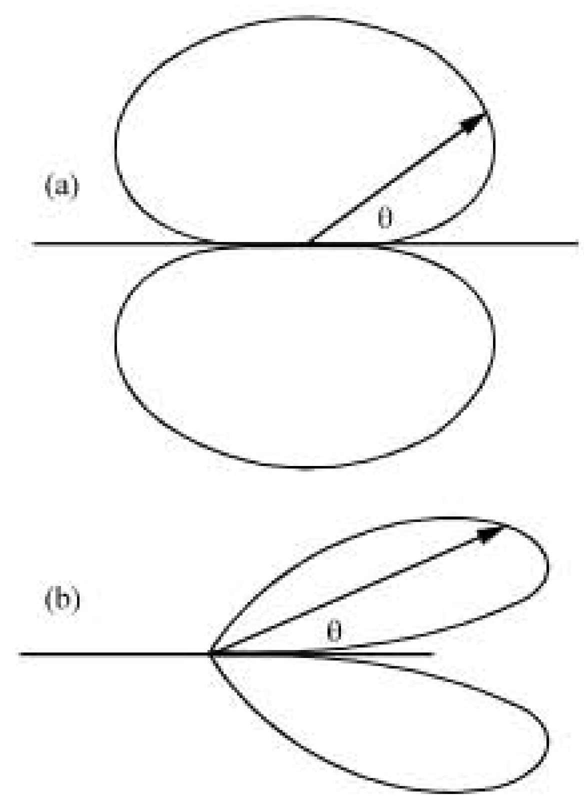

Fig. 4: Diffuse and deterministic radiation patterns, (a) vDiffuse element pattern (Lambert's law) and (b) Deterministic element pattern at 900 MHz

solid angle from a thin Lambert's law cable element is proportional to sin(θ), where θ is the angle between the viewing direction and the cable axis. The equivalent electrical field E, generated at distance, r by a thin cable element is proportional to (Morgan, 1998):

$$E = S(\theta)/r, \qquad S(\theta) = \sqrt{\sin(\theta)} \tag{1}$$

where, S(θ) is shown in Fig. 4a.

Deterministic model: In the deterministic model, radiating mode cable is considered as an array of coherent point source. If we assume each period of existing slots as an independent radiating source, the field pattern of a source can be found as follows:

$$E = S(\theta)/r, \qquad S(\theta) = S_0(\theta)\, S_1(\theta) \tag{2}$$

where, $S_0(\theta)$ and $S_1(\theta)$ are the pattern of a single slot and the array factor of a single period of the slot sequence, respectively. Figure 4b shows a plot of the product $|S_0S_1|$ of the slot and array patterns at 900 MHz (Morgan, 1998). Hence, we will be considering the electric field at large distance by applying the slot pattern.

MODIFIED RAY TRACING ALGORITHM

This algorithm is a method for estimating the path of wave propagation characteristics through a cellular environment. In this algorithm, the transmitted (i.e., radiating) wave is modeled by a series of rays and wave propagation is simulated by tracing them.

When applied to problems of electromagnetic radiation, ray tracing often relies on approximate solutions to Maxwell's equations that are valid as long as the light waves propagate through and around objects whose dimensions are much greater than the light's wavelength. However, there are also challenges with the use of ray theory, specifically, whit phenomena such as interference and diffraction, which require wave theory (involving the phase of the wave). Hence, we modify the algorithm as following steps.

Angular rays resolution: Ray tracing operates by supposing that the particle or wave can be modeled as a large number of very narrow beams (i.e., rays) and that there exists some (possibly very small) distance over which such a ray is locally straight. The ray tracer will advance the ray over this distance and then use a local derivative of the medium to calculate the ray's new direction. From this location, a new ray is sent out (i.e., distributes) and the process is repeated until a complete path is generated. If the simulation includes solid objects, the ray may be tested for intersection with them at each step, making adjustments to the ray's direction if a collision is found as shown in Fig. 5. Other properties of the ray may be altered as the simulation advances as well, such as intensity, wavelength, or polarization.

To avoid discrete errors of wave front due to interference and diffraction through another rays as well as propagation modeling errors, database and kinematic errors, it is necessary that the transmitted rays to be together. In other word, angular resolution of rays is high (i.e., high-resolution). Hence, the numbers of transmitted rays become extremely and the program execution requires more time that is directly proportional to the number of these rays increases. Hence, we obtain the angular rays resolution (ARE), as shown in Fig. 6:

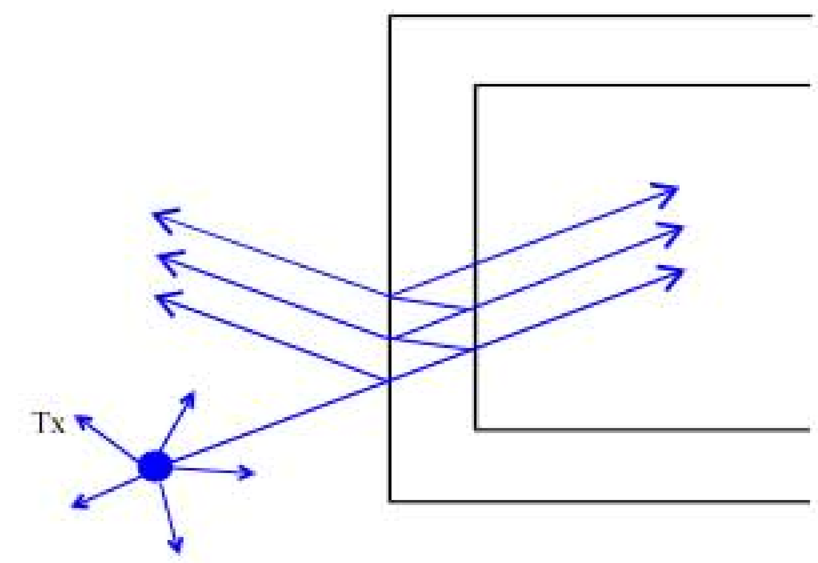

Fig. 5: Illustration of the penetrate obstacle (Snell law)

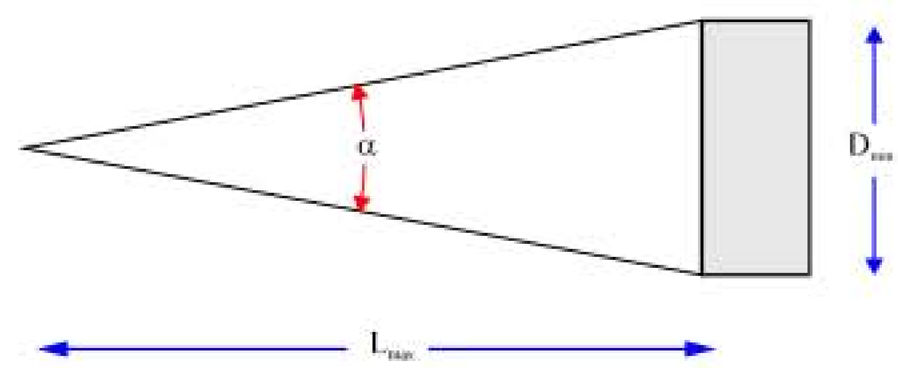

Fig. 6: Illustration of the ray's angular resolution

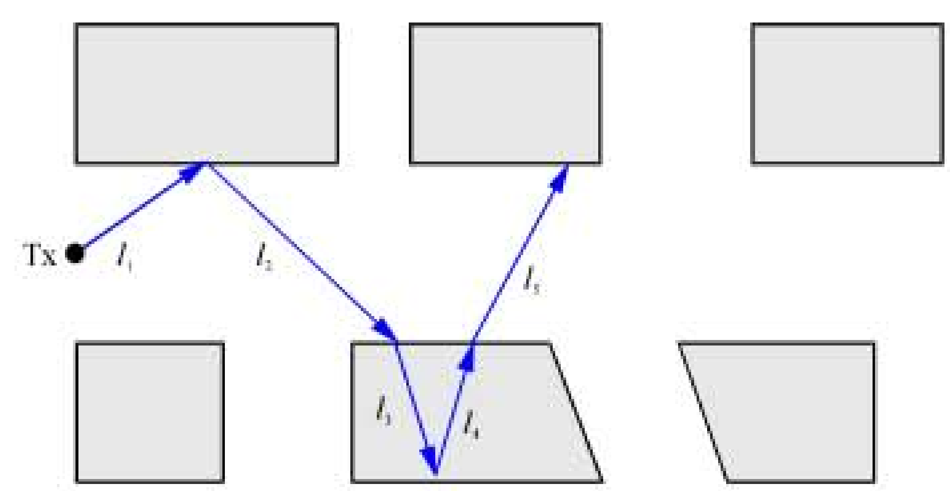

Fig. 7: Geometry of the ray propagation model

$$\alpha = 2\tan^{-1}\left(\frac{D_{min}}{2L_{max}}\right) \tag{3}$$

where, D_{min} is minimum dimension of obstacle and L_{max} is the maximum trajectory of ray propagation among of all possible paths, p, up to ray tracing terminate as demonstrated in the next subsection. For instance we compute the L_{max} as shown in Fig. 7 (e.g., m = 5):

$$L_{tr} = \sum_{i=1}^{m} L_i, \qquad L_{max} = \max_{p}\{L_{tr}\} \tag{4}$$

where, m is the number of the rays in a certain path (i.e., contain transfer, reflection and refraction rays). To avoid computational complexity in Eq. 4, due to complexity concerning n, let us consider the case of L_{max} according to transmit and threshold powers.

Further improvements can be achieved by assigning different phenomenon to receiver power as follows (Chen and Jeng, 1996):

$$P_r = P_t\left(\frac{\lambda}{4\pi L}\right)^2 \tag{5}$$

where, L is the distance between transmitter and receiver and λ is the wavelength in free space, P_t and P_r are transmitted and received power, respectively. The L_{max} can be expresses as:

$$L_{max} = \left(\frac{\lambda}{4\pi}\right)\sqrt{\frac{P_t}{P_{th}}} \tag{6}$$

where, P_{th} is the minimum acceptable power at the receive side.

The procedure of modified ray tracing algorithm: Other procedural problem due to mentioned algorithm is tracing error (i.e., criterion of ray tracing termination). The conventional algorithm terminates the ray tracing according to Trace Indicator (TI) of the propagation mechanisms (i.e., reflection, transmit, refraction). Obviously, this procedure seems to be logically with performance degradation due to termination of the rays having significant power. For instance, we assume the TI equal to there, the second ray power is large than the first ones, due to path loss method, as shown in Fig. 8. Therefore, we proposed a criterion in related to trace termination which is operates by computing Ray's Power (RP) in each incidence and is compared with Threshold Power (TP) (i.e., minimum acceptable signal-to-noise ratio level). The ray tracing is continued only whereas the RP to become more than the TP.

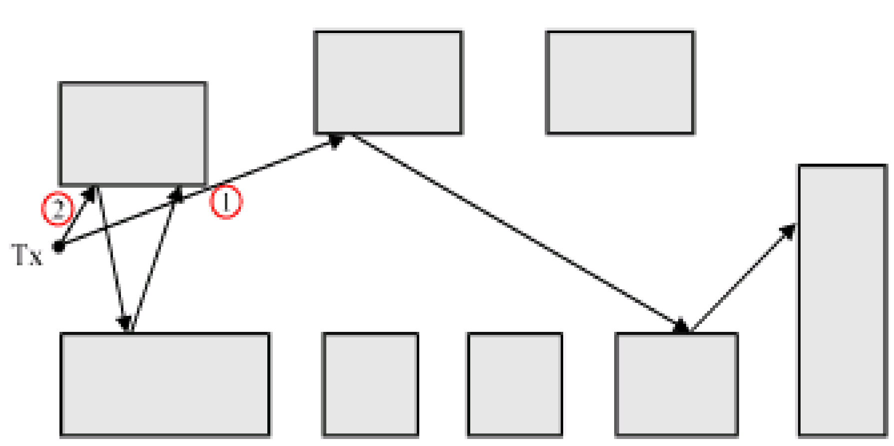

Fig. 8: Criterion of ray tracing termination

ELECTROMAGNETIC PROPAGATION PROCESSES

After finding of direction by ray tracing algorithm and to be found of rays that have begun from transmitter and have reached receiver with one or several propagation processes, for calculation of received power at receiver it is necessary to have the power of one by one of received rays and it is impossible except with calculation of loss for each one of happened propagation processes on the way of ray.

Reflection and transmission: Theories for calculation of reflection and transmission coefficients have reported by Chen and Jeng (1996), Kermani *et al*. (2000) and Landron *et al*. (1996). For example, to calculate the reflection coefficient, in some cases a constant coefficient has been used, while other cases used the type of obstacle and incidence angle. The used reflection and transmission coefficients at computer program are different for two kind of polarization and depend on the kind of obstacle, wavelength and incidence angle. These coefficients depend on the surfaces characteristic among flat and smooth completely at working frequency. For high frequencies that are used in mobile communication, the obstacles surfaces such as buildings wall are not smooth completely and so scattering effect is seen also at reflected rays from surfaces. This effect will reduce the reflection coefficient and this reduction is very sensible when surface roughness is in limit of one wavelength or more. In general if the variations of surface are more than the limit of threshold that is obtained by following relation, the effect of surface roughness must be considered (Kermani *et al*., 2000):

$$h_R = \frac{\lambda}{8\sin\psi} \tag{7}$$

where, λ and ψ are the incidence wavelength and the angle of incidence to the surface, respectively. So, as result of surface roughness, the reflection coefficient of smooth surfaces is modified in following:

$$\Gamma_{Rough} = \rho\Gamma_{Smooth} \tag{8}$$

where, ρ can be obtained from the following Eq. 9:

$$\rho = \sqrt{\exp\left(\frac{-8\pi\sigma_h}{\lambda}\sin\psi\right)} \tag{9}$$

where, σ_h is standard deviation of the surface variance. The surface roughness causes to generation of scattered rays also in addition the amplitude decrease of reflection basic part (Chen and Jeng, 1996) and (Landron *et al*., 1996). The scattered rays amplitude, E_{sc} can be found as:

$$E_{sc} = E_{sp}\frac{1}{h}\left[\%1\frac{2\pi\sigma_h}{\lambda}\cos\left(\frac{\Delta\phi}{2}\right)\right] \tag{10}$$

The amplitude of main reflection component denoted by E_{sp} also $\Delta\phi$ is the difference angle between the scattered and the reflection rays and E_{sc} is the maximum surface variation.

Received power: After transmission of the total rays from transmitter and tracing of them, the number of ray is received with powers $P_1, P_2,...,P_n$ after traveling through of distances $L_1, L_2,...,L_n$ and with phases $\phi_1, \phi_2,...,\phi_n$ by receiver. The total received field intensity can be obtained as follows (Chen and Jeng, 1996):

$$E_{total} = \sum_{i=1}^{n} E_i e^{j\phi_i} e^{jk_0 L_i}$$

$$L_{dB} = 20\log|E_{total}| \tag{11}$$

where, k_0 is the wave number in the free space, the ratio of field intensity from the received components to transmitted field intensity denoted by E_i and L_{dB} is the path loss. It is considerable that the phase of received rays must be considered also in calculation of E_{total}. The algorithm also inability the forecast of fast fading, in case of apart from phase in addition to the quantity of error in path loss estimation. In this implementation, the leaky cable system becomes as distributed antenna in tunnel longitude. Hence, to compute received power should be calculate the radiation power from every array of slots whit pattern consideration as transmitter. Then, we apply the modified ray tracing algorithm to each slot sets, afterwards the electromagnetic propagation process can be executed. Let us recall Eq. 2, slot pattern $S_0(\theta)$ can be obtained as follows (Morgan, 1998):

$$S_0(\theta) = \frac{C_0}{xH_0^{(2)}(x) + \Delta H_1^{(2)}(x)} \tag{12}$$

where, C_0 is a constant that proportional to the wave incident field in the cable (i.e., $C0 \cong NV_0$ and integer number 1~4). The Hankel functions are denoted by H's. Other parameters are defined in following:

$$k = \frac{2\pi}{\lambda},\ \Delta = k^2bt\left[\frac{1-\cos^2(\theta)}{\varepsilon_s}\right], \tag{13}$$
$$x = kb\sin(\theta)$$

where, b, t and ε_s are the outer conductor radius, thickness of the coverage dielectric and constant of the coverage dielectric, respectively. We can obtain relationship of the S_0 whit potential difference, V_0 between inner and outer conductor in the coaxial cable.

$$V_0 = \sqrt{\frac{50P_{in}}{\pi}\ln\left(\frac{b}{a}\right)} \tag{14}$$

where, P_{in} is the input power to the cable a and b are inner and outer radius of the cable. Then the electric field at large distance can be determined as (Morgan, 1998):

$$E_\theta = \frac{S_0(\theta)\exp(-jkr)}{r} \tag{15}$$

Computation of radiating pattern concerning leaky coaxial cable deployment: We consider leaky coaxial cable deployment (LCXD) as shown in Fig. 9. The cable illustrated by four slot sets, each set also contains fifteen up to eighty slots and every slot has certain dimensional stability (e.g., generally 1.2×0.2 mm) as well as slot spacing (e.g., 0.5 mm). These four slot sets located on cable circumference with overall length approximate to λ.

Let us compute radiating field of LCXD as follows:

Step 1: For one slot set (e.g., n = 15 in Fig. 9), compute array factor
Step 2: For two slot sets are situated one side (e.g., solid slots in Fig. 9), compute equivalent array factor
Step 3: For step 2, compute subtotal array factor
Step 4: For two slot sets in opposite direction, obtain subtotal array factor as mentioned in step 3
Step 5: Finally, compute total radiating field

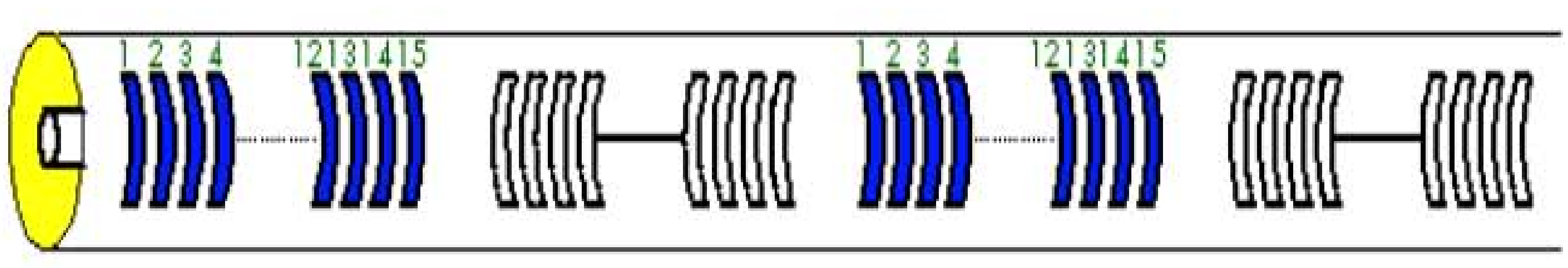

Fig. 9: Illustration of the LCXD with n = 15 and 4 slot sets

As mentioned earlier, the radiating array field on direction of axis z, can be written as follows (Landron *et al*., 1996):

$$\bar{E}_1 = \left(1 + e^{j\psi} + e^{2j\psi} + ... + e^{j(n-1)\psi}\right)\bar{E}_0$$
$$\psi = \frac{2\pi d}{\lambda_0}\cos\theta + \delta,\ \delta = \frac{2\pi d}{\lambda},\ \lambda = \frac{\lambda_0}{\sqrt{\varepsilon\gamma}}$$

where, d is the slot spacing. From this, we can show that:

$$\bar{E}_1 = e^{j\zeta}\frac{\sin(n\psi/2)}{\sin(\psi/2)}\bar{E}_0,\quad \zeta = \frac{(n-1)}{2} \tag{16}$$

Where:
$\bar{E}_0 = E_\theta l(n-1) \leftarrow n$

To compute subtotal array factor, the resulting in Eq. 16 yields as:

$$\bar{E}_{st} = \bar{E}'_1 + \bar{E}'_1 e^{j\psi'} \tag{17}$$

$$\psi' = \frac{2\pi d'}{\lambda_0}(\sqrt{\varepsilon\lambda} + \cos\theta) \tag{18}$$

The distance between two arrays in the same direction is given by d'. According to our implementation, d' = λ/2 Eq. 18 becomes as:

$$\psi' = \pi\left(1 + \frac{\cos\theta}{\sqrt{\varepsilon_\gamma}}\right)$$

Consequently, we can apply analogous process concerning step 4.

SIMULATION RESULTS

We use the same simulation setup as in (Kim *et al*., 2006; Landron *et al*., 1996). In this implementation, the results are obtained with some details as shown in Fig. 10 and the input power supposed equal to one watt. The signal received level also computed by considering of the path loss and speed of propagation.

Simulations are performed in three steps:

- Firstly, we compare radiating pattern in terms of frequency, f and slot number, n in each array. In Fig. 11, the received power can be increased while f and n enhanced. Due to the focusing effects of the arched tunnels which results in constructive interference and mitigate the deep fading, the received power inside the arched tunnel is superior to the rectangular tunnels. This step provides some trade-off between f and n, which is needed in certain applications
- Secondly, we focus on the received signal level. Figure 12 and 13 show the curves in terms of dB_m versus f. We note that the fading is less strict in the arched tunnels as compared to the rectangular tunnels also when f increase, a significant enhance in coverage can be observed as compared to (Kim *et al*., 2003) (about 5.99 dB). Hence, the LCXD radio system is investigated as efficient solution from an economical standpoint for frequencies up to 2 MHz
- At the final step, we keep f = 925 MHz in a rectangular tunnel. According to simulation results as shown in Fig. 14-16; we consider that when f increased (e.g., n = 86) a drastic enhance in coverage can be obtained whereas a slight decrease in the received signal level can be observed (about 0.8 dB)

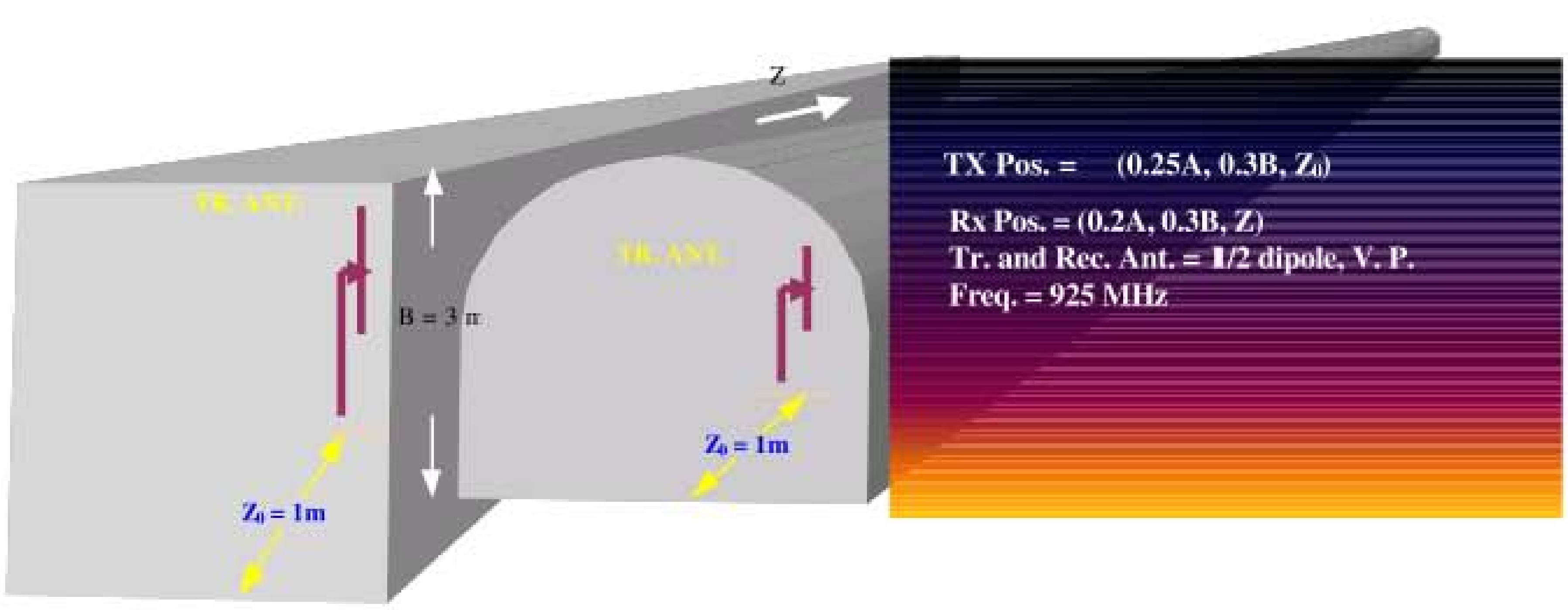

Fig. 10: Illustration of the rectangular (A = 7.5 m, B = 4 m) and arched (A = 6.4 m, B = 4 3) tunnels

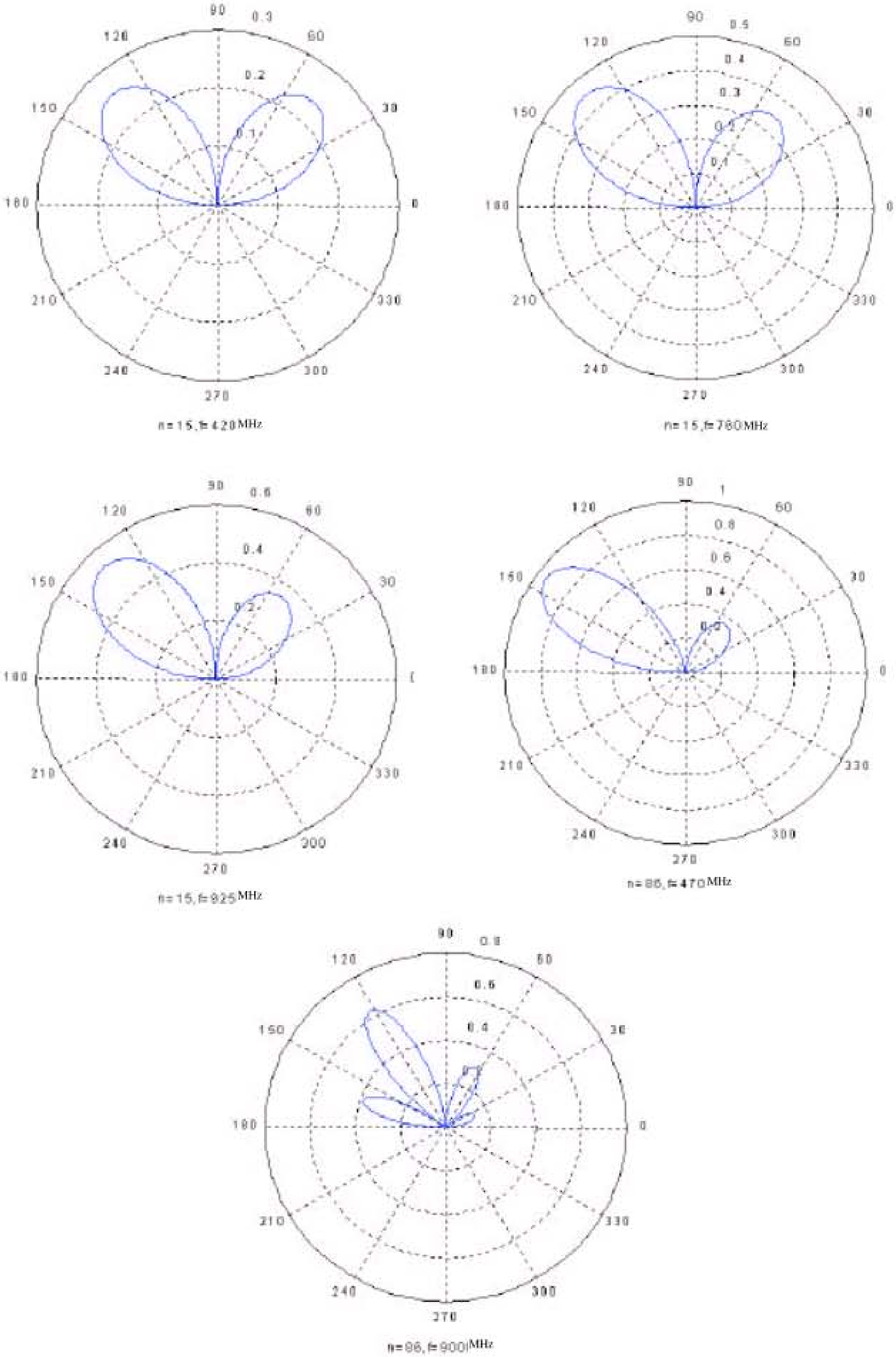

Fig. 11: Radiation patterns at frequencies and slots whit polar coordinate

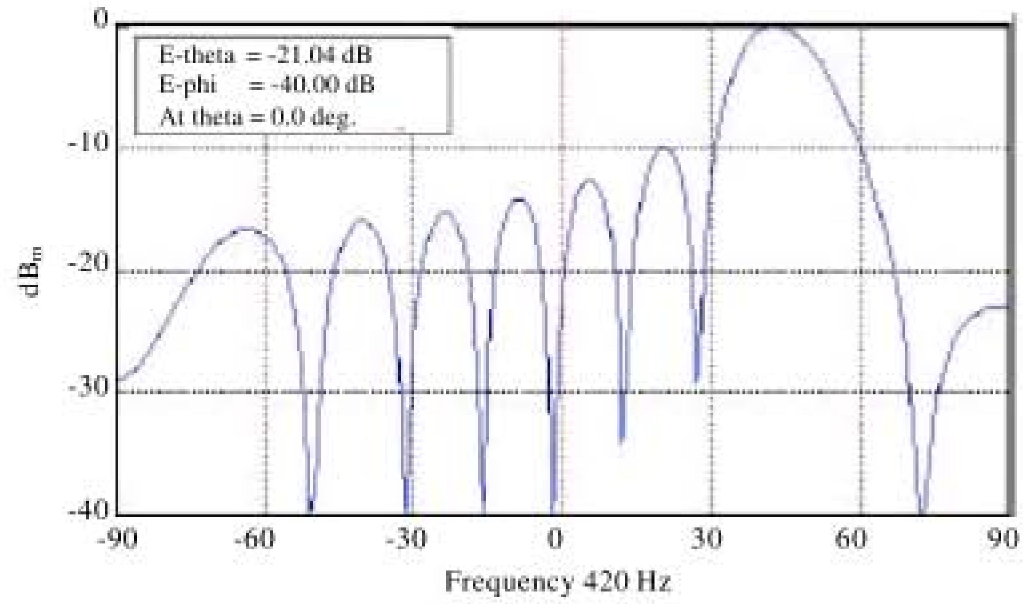

Fig. 12: Simulation result in an equivalent arched tunnel at 420 MHz

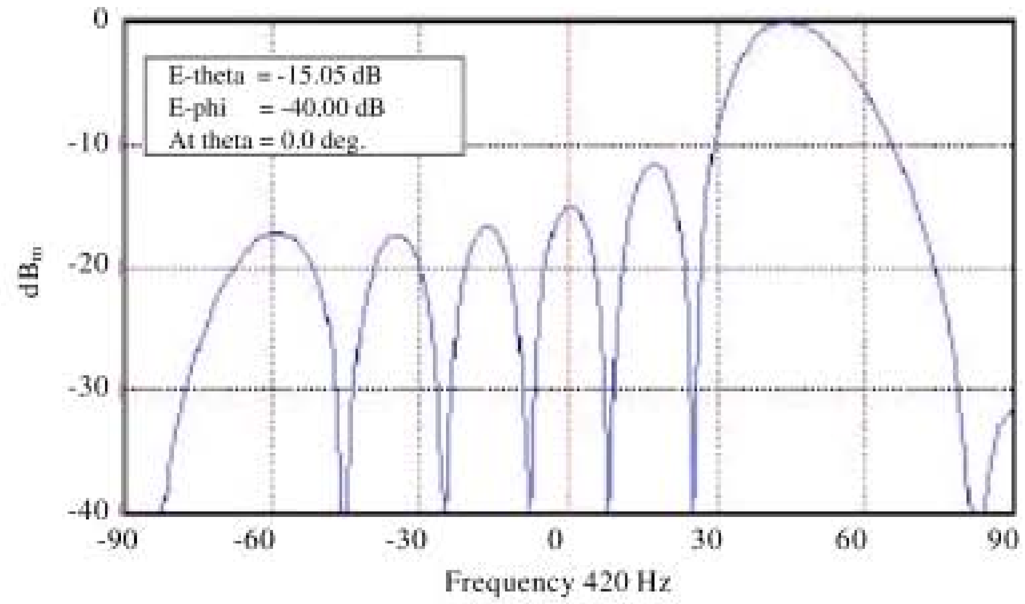

Fig. 13: Simulation result in an equivalent arched tunnel at 925 MHz

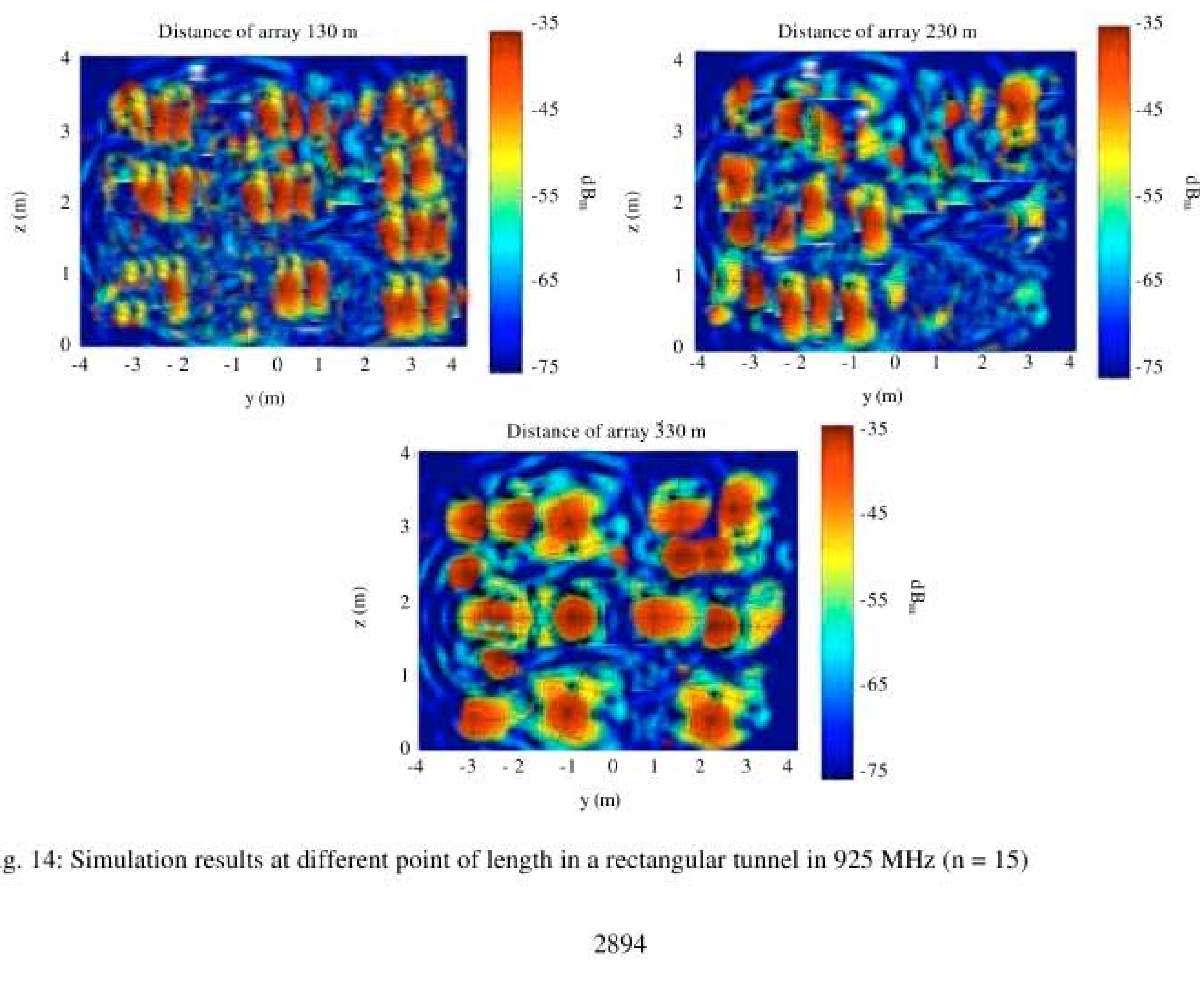

Fig. 14: Simulation results at different point of length in a rectangular tunnel in 925 MHz (n = 15)

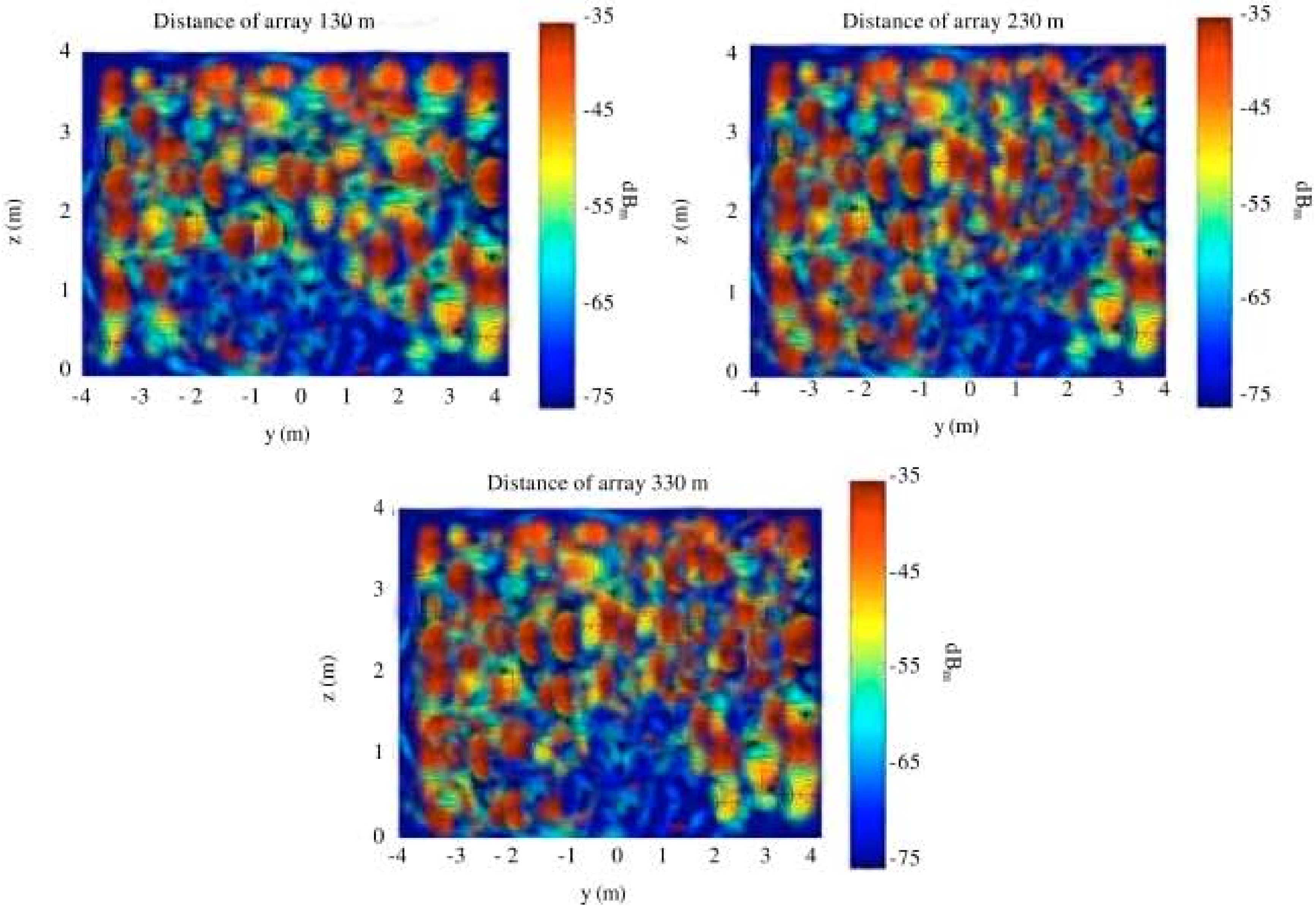

Fig. 15: Simulation results at different point of length in a rectangular tunnel in 925 MHz (n = 86)

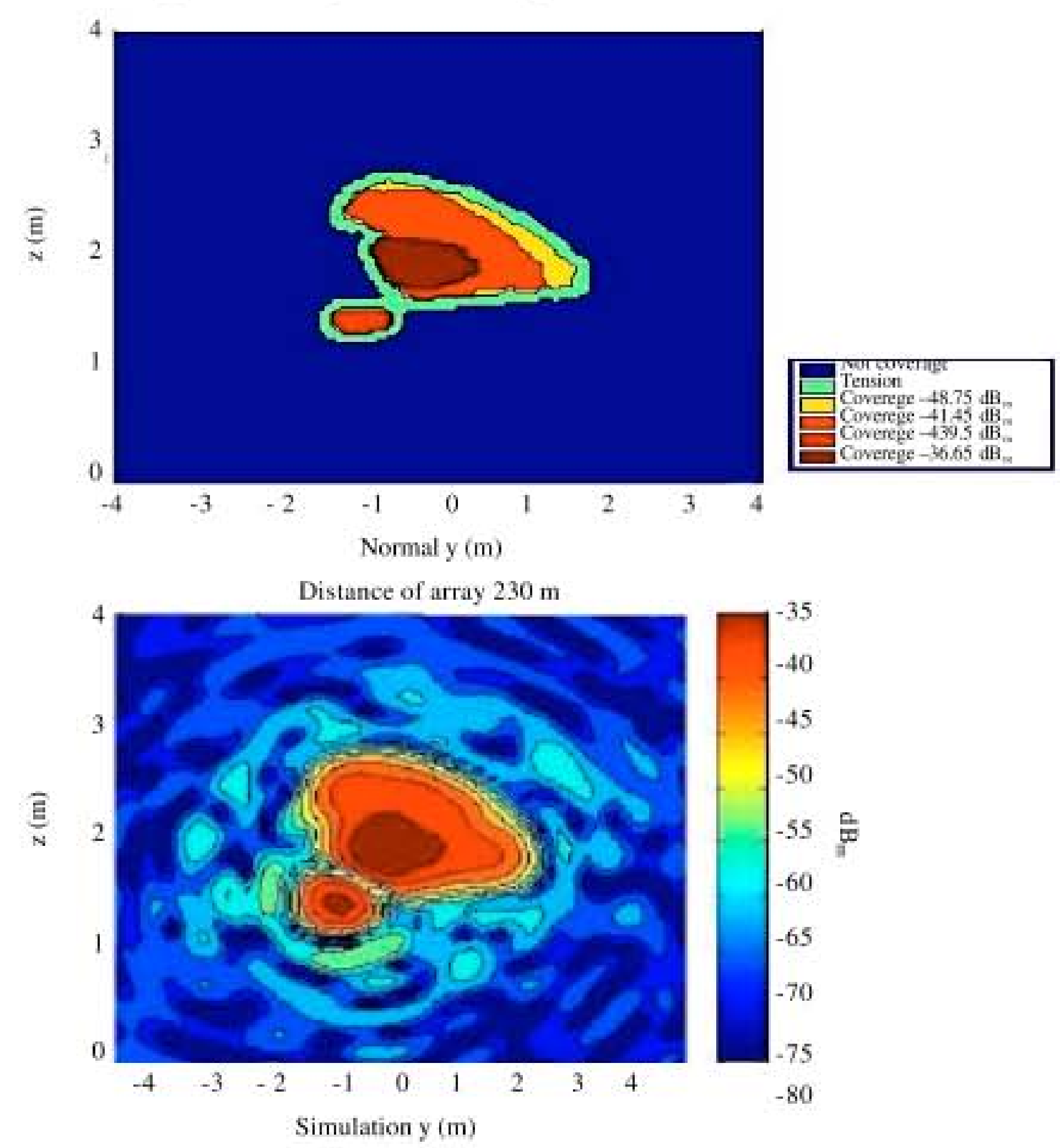

Fig. 16: Simulation results in cross section of a rectangular tunnel in 925 MHz

CONCLUSION

We have presented the radio coverage applying leaky coaxial cable deployment (LCXD) as an alternative to the distributed antenna for wireless links in a complex environment as tunnels. The modified ray tracing algorithm is proposed to radio coverage estimation in tunnels by LCXD. To achieve high accuracy, we have been computed the angular rays resolution in terms of the transmitted and threshold powers. We also defined drastic criterion of ray tracing termination. In this study, the radiation characteristics of the LCXD with general slots are studied by a hybrid method that involves the Geometric optics method for the near-field computation and the mode deterministic method for the transformation of near field to far field. Present new method allows having the capability of modifying the coupling between the cable and the environment and give smoother electric field coverage. We have shown that LCXD achieves better RF coverage than distributed antennas, at different point of length and cross section that is validated by simulation results.

ACKNOWLEDGMENT

The authors would like to acknowledge the support of the Malaysian Ministry of Science, Technology and Innovation for funding this research work under project code: UKM-GUP-NBT-08-29-120.

REFERENCES

Addamo, G., R. Orta and R. Tascone, 2008. Bloch Wave analysis of long leaky coaxial cables. IEEE Trans. Antennas Propagat., 56: 1548-1554.

Chen, S.H. and S.K. Jeng, 1996. SBR image approach for radio wave propagation in tunnels with and without traffic. IEEE Trans. Vehicular Technol., 45: 570-578.

Kermani, M.H. and M. Kamarei, 2000. A ray-tracing method for predicting delay spread in tunnel environments. Proceedings of the IEEE International Conference on Personal Wireless Communications, Jun. 12-17, Hyderabad, India pp: 538-542.

Kim, Y., M. Jung and B. Lee, 2003. Analysis of radio wave propagation characteristics in rectangular road tunnel at 800 MHz and 2.4 GHz. Proceedings of the IEEE International Symposium on Antennas and Propagation Society, Jun. 22-27, South Korea, pp: 1016-1019.

Landron, O., M.J. Feuerstein and T.S. Rappaport, 1996. A comparison of theoretical and empirical reflection coefficients for typical exterior wall surfaces in a mobile radio environment. IEEE Trans. Antennas Propagat., 44: 341-351.

Morgan, S.P., 1998. Prediction of indoor wireless coverage by leaky coaxial cable using ray tracing. Proceedings of the 48th IEEE Vehicular Technology Conference, May 18-21, Ottawa, Ont., Canada, pp: 591-595.

Yamaguchi, Y., T. Abe, T. Sekiguchi and J. Chiba, 1985. Attenuation constants of UHF radio waves in arched tunnels. IEEE Trans. Microw. Theory Techniques, 33: 714-718.